International Journal of Emerging Science and Engineering (IJESE)
ISSN: 2319–6378 (Online), Volume-13 Issue-7, June 2025

Systematic Simulation and Characterization of LLC Resonant Converter Operating Regions

Sushil Bhartoon, Tanmay Dharma, M.P.S. Chawla, Khushboo Nagar

***Abstract:** This paper presents an LTspice simulation study investigating the operational characteristics of an LLC resonant converter across its three distinct operating regions: at, above, and below the resonant frequency. This research aims to comprehensively understand the converter's behaviour, which is essential for optimising its design and performance in power electronic applications such as telecommunications, data centres, and Electric Vehicle charging. The methodology involved detailed analysis of key waveforms—inductor currents, output voltage, and diode currents under controlled frequency variations, with simulations conducted at 300 kHz, 459 kHz (resonant), and 600 kHz. Discoveries show that resonant operation yields favourable soft-switching, while deviations, especially those occurring below resonance, increase component stress and lead to harder diode switching and higher peak currents. The phase relationship between magnetizing and resonant inductor currents indicates the operating regime. Despite varying switching conditions, excellent output voltage regulation was consistently maintained. These findings provide valuable insights into the trade-offs between operating frequency, component stresses, and switching losses, affirming that operating near resonance offers an optimal balance.*

***Keywords:** LLC Converter, Resonant Frequency, switching frequency, Inductor Current, Diode current, ZVS, ZCS*

Abbreviations:
fs: Switching Frequency
fr: Resonant Frequency
Lm: Magnetizing inductor
Lr: Resonant Inductor
Cr: Resonant Capacitor
ZCS: Zero Current Switching
ZVS: Zero Voltage Switching

I. INTRODUCTION

The LLC resonant converter has become a popular choice in various power electronic applications, including telecommunications, data centres, and electric vehicles.

Manuscript received on 23 May 2025 | First Revised Manuscript received on 26 May 2025 | Second Revised Manuscript received on 04 June 2025 | Manuscript Accepted on 15 June 2025 | Manuscript published on 30 June 2025.
*Correspondence Author(s)

Sushil Bhartoon*, Department of Electrical Engineering, Shri G.S. Institute of Technology and Science, Indore, (M.P.), India. Email ID: sushilbhartoon@gmail.com, ORCID ID: 0009-0004-0134-9826

Tanmay Dharma, Department of Electrical Engineering, Shri G.S. Institute of Technology and Science, Indore, (M.P.), India. Email ID: dharma.tanmay21@gmail.com

Prof. M.P.S. Chawla, Department of Electrical Engineering, Shri G.S. Institute of Technology and Science, Indore, (M.P.), India. Email ID: mpschawla@gmail.com,

Khushboo Nagar, Assistant Professor, Department of Electrical Engineering, Shri G.S. Institute of Technology and Science, Indore, (M.P.), India. Email ID: knagar@sgsits.ac.in, ORCID ID: 0000-0002-4111-8983

Charging, owing to its advantages, such as a wide input voltage range, high efficiency, and high-power density [8].

These attributes make it particularly well-suited for systems that demand a compact size and minimal energy loss.

A key feature of the LLC resonant converter is its operation based on frequency modulation, which allows it to function in three distinct operating regions: at, above, or below the resonant frequency [7]. Each region exhibits unique electrical characteristics and performance trade-offs [10]. Therefore, a comprehensive understanding of the LLC resonant converter's behavior in these different operating regions is paramount for optimizing its design, control, and overall system performance [9].

This paper presents a detailed investigation into the operational characteristics of the LLC resonant converter through simulation. The study systematically analyses the key waveforms, including inductor currents, output voltage, and diode currents, as well as performance metrics in each of the three operating regions. By examining the converter's behavior under varying frequency conditions, this work aims to provide valuable insights into the inherent trade-offs between operating frequency, component stress, switching losses, and overall efficiency. The simulation results offer a basis for informed design decisions and developing control strategies in LLC resonant converter applications [1].

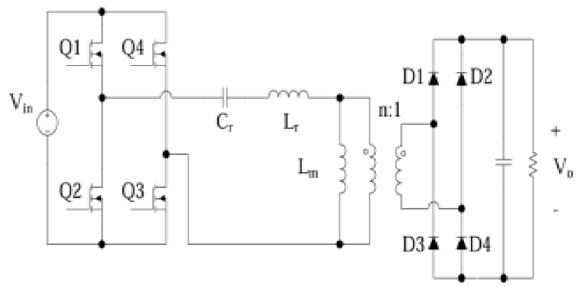

[Fig.1: Bridge LLC Resonant DC-DC Converter [10]]

II. REGIONS OF OPERATIONS OF LLC RESONANT CONVERTER

The LLC converter's operational modes are determined by frequency modulation of its network gain, allowing it to function within three distinct regions based on input voltage and load current [6].

At resonant frequency fs=fr.

Above resonant frequency fs>fr.

Below Resonant frequency fs<fr.

Despite the three modes referenced earlier, which will be elaborated on later in this section, the converter performs only two types of operations during each switching cycle. Each of the previously mentioned modes may involve one or both operations.

A. Power Transfer Operation

In a resonant converter, power is transferred twice per switching cycle. Initially, positive voltage energizes the resonant tank, causing current to flow positively [Figure-1(A)]. Subsequently, a negative voltage excites the tank, leading to current resonance in a negative direction [Figure-1(B)] [12]. Throughout this operation, the magnetizing inductor's voltage swings between positive and negative reflected output voltages, and its current charges and discharges accordingly [12]. Power is delivered to the secondary side and ultimately to the load through the transformer and rectifier, with the net power being the consequence of the divergence between the resonant and magnetizing currents.

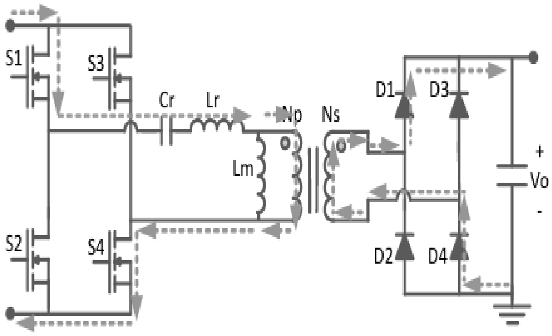

(A)

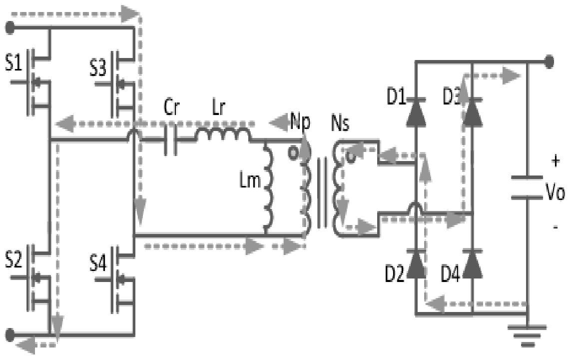

(B)

[Fig.2: (A) & (B) Power Transfer Operation [12]]

B. Freewheeling Operation

After power delivery, freewheeling is initiated because the current flowing through the resonant inductor matches the transformer's magnetizing current. This condition is met when the switching frequency (fs) is below the resonant frequency (fr), causing the secondary current to drop to zero and the rectifier to disconnect [4]. At this point, the magnetizing inductor interacts with the resonant inductor and capacitor, forming secondary resonance [(Figure-2(A)] [12]. The frequency of this resonance is below than the primary resonant frequency (fr), especially when the magnetizing inductance (Lm) is significantly larger than the resonant inductance (Lr). During this phase, the primary current remains nearly constant [Figure-2(B)], allowing it to be approximated as unchanged for simplicity.

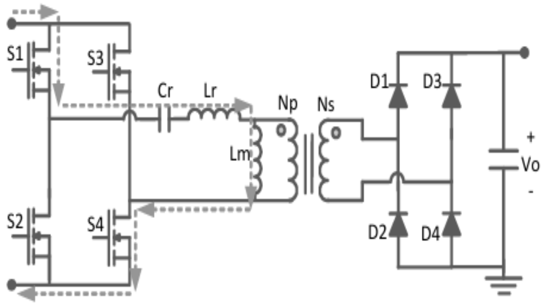

(A)

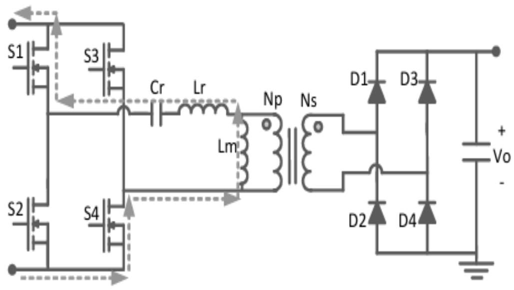

(B)

[Fig.3: (A) & (B) Freewheeling Operation [12]]

C. At Resonant Frequency(fs=fr)

Power is transferred during each half of the switching cycle, with the resonant behaviour synchronised to the switching period as shown in Figure-3 [12]. By the conclusion of each switching half-cycle, the current flowing through the resonant tank (I_{Lr}) converges with the magnetizing current (I_{Lm}), and the rectifier current diminishes to zero. The resonant tank exhibits unity gains at this point, contributing to optimal efficiency and operation. Effective performance at this defined operating point relies on the transformer's turns ratio, which is precisely selected for nominal input and output voltage conditions [4].

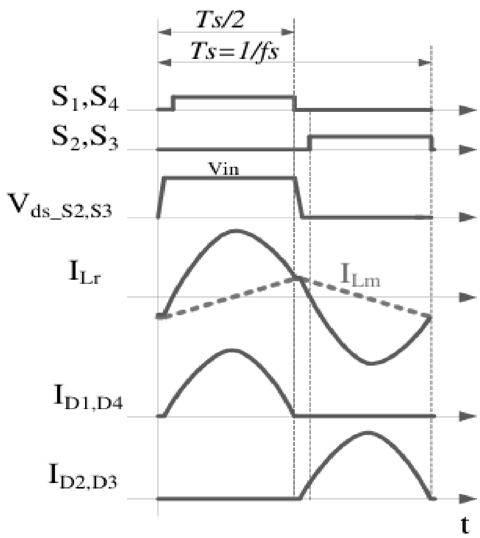

[Fig.4: Typical Waveform of LLC Converter at Resonance Frequency [12]]

Retrieval Number:100.1/ijese.G260713070625
DOI:10.35940/ijese.G2607.13070625
Journal Website: www.ijese.org

Published By:
Blue Eyes Intelligence Engineering
and Sciences Publication (BEIESP)

D. Above Resonant Frequency (fs>fr)

A partial power transfer occurs (as described earlier), resembling resonant operation during each switching half-cycle. However, unlike a complete resonant cycle, the process is interrupted before completion by the onset of the next half-cycle, as shown in Figure 4. As a result, the primary-side MOSFETs experience increased turn-off losses, and the secondary rectifier diodes undergo hard commutation. This operating condition typically occurs at higher input voltages, where the converter functions in a step-down or buck-like mode [4].

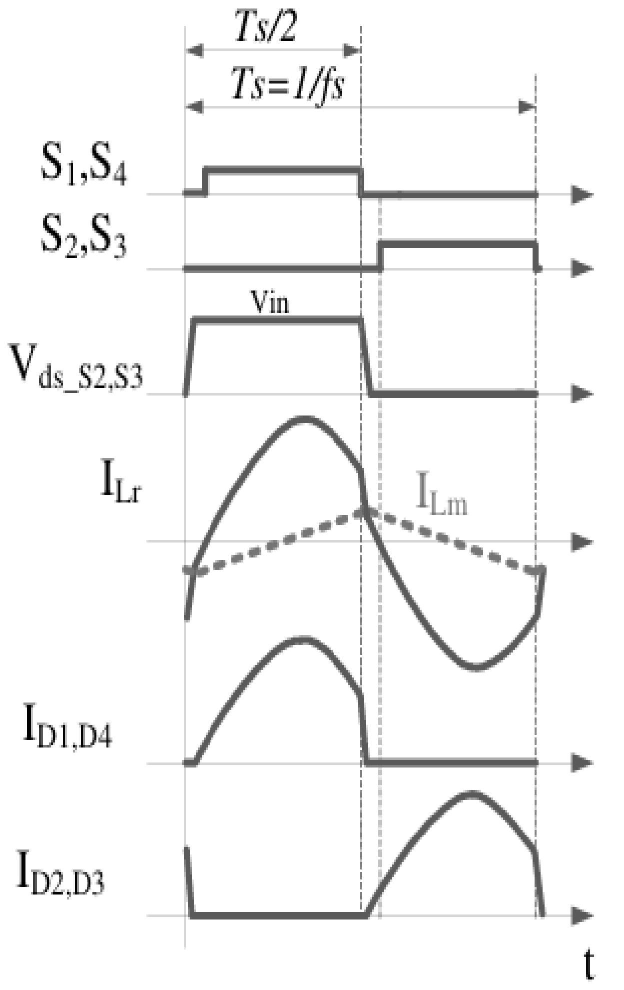

[Fig.5: Typical Waveform of LLC Converter Above Resonance Frequency [12]]

E. Below Resonant Frequency (fs<fr)

During each half of the switching cycle, power is transferred as part of the process described earlier. Once the resonant half-cycle completes and the current flowing through the resonant tank (I_{Lr}) matches the magnetizing current (I_{Lm}The converter enters a freewheeling phase (also previously described) that continues until the end of the switching interval, as shown in Figure 5. This increases conduction losses on the primary side due to circulating energy. The converter typically operates in this mode under low input voltage conditions, where step-up or boost-like behavior is required [4].

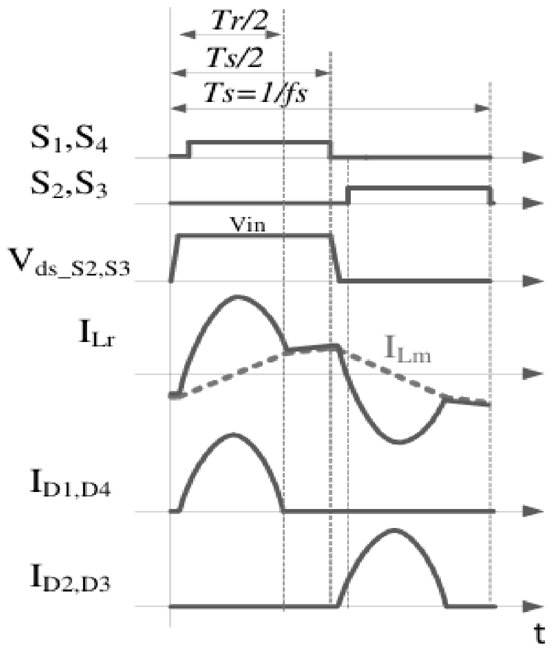

[Fig.6: Typical Waveform of LLC Converter Below Resonance Frequency [12]]

III. SIMULATION AND RESULTS

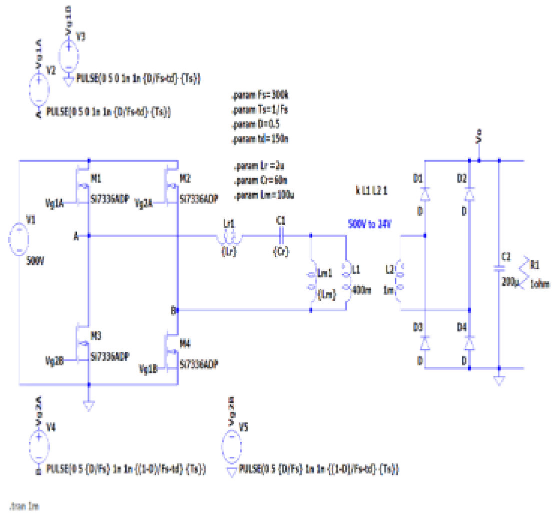

[Fig.7: LTspice Model of Converter at Resonant Frequency [13]]

Fig. 6 presents the LTspice model of the resonant LLC converter, a widely used topology for DC-DC power conversion due to its high efficiency and soft-switching capabilities. The circuit features a full-bridge inverter (M1-M4) driving a resonant tank (Lr, C1, Lm1, Lm2) which, through a high-frequency transformer, provides isolation and voltage step-down from 500V to 24V. The output stage employs a full-bridge rectifier (D1-D4) followed by an LC filter (C2, R1) to produce a smooth DC output. This model was utilized to investigate the converter's performance across various operating regions, with simulations conducted at switching frequencies of 300 kHz, 459 kHz and 600 kHz to assess their impact on key characteristics [11].

Published By:
Blue Eyes Intelligence Engineering
and Sciences Publication (BEIESP)

Table-I: Parameters of the LTspice Model of the LLC Converter [13]

Parameters	Specifications
Input Voltage	500V
Output Voltage	24V
Resonant Inductor (Lr)	2µH
Resonant Capacitor (Cr)	60nF
Magnetizing Inductor (Lm)	100µH
Resonance Frequency(fr)	459.4kHZ
Output Power	476W

A. At Resonant Frequency (fs=fr=459kHz).

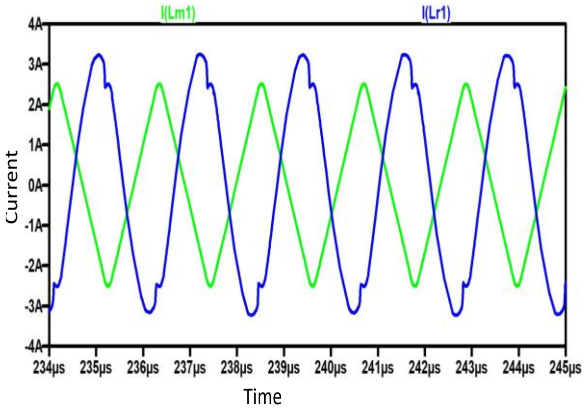

[Fig.8: Inductors Current Waveform of Converter at the Resonance Frequency]

Both are inductor currents, but their waveforms differ significantly, as shown in Figure-7. I(Lm1) exhibit a roughly triangular shape with rounded peaks, directly influenced by the primary MOSFET switching action. In contrast, I(Lr1) display a roughly sinusoidal waveform with flattened peaks, both shapes resulting from the LLC converter's resonant operation at the switching frequency. The peak positive current for I(Lm1) is approximately 2.6A, while I(Lr1) reaches around 3.4A; these amplitudes are contingent on the input voltage, load, and the resonant network parameters (Lr, Lm, &Cr). Observing their phase relationship, the I(Lm1) peaks lag those of I(Lr1), meaning the green waveform's peaks occur slightly after the blue waveform's peaks. Both waveforms share an approximate period of 2.18µs, resulting in an approximate frequency of 459 kHz, indicating they oscillate at the same rate.

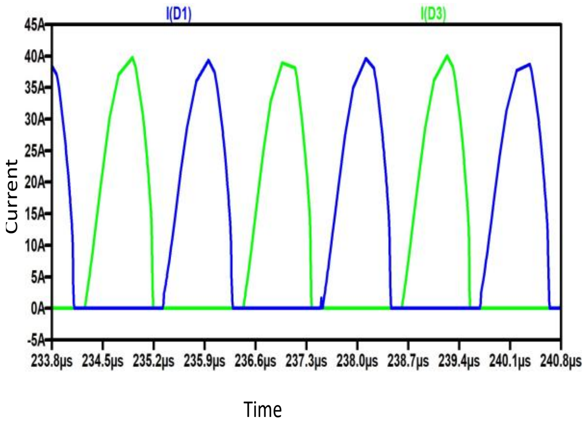

[Fig.9: Diode Waveform of Rectifier at Resonant Converter]

The simulation of the rectifier stage as shown in Figure-8, reveals balanced operation between diodes D1 (blue) and D3 (green). Each diode conducts for approximately 1.09µs per cycle, representing half of the total switching period (T ≈ 2.18µs), and exhibits a high peak current of around 40A, characteristic of high-power resonant converters. Both diodes operate at the resonant frequency of 459kHz and conduct alternately, typical of a center-tapped full-wave rectifier configuration, each experiencing a non-conduction interval of approximately 1.09µs. This results in a 50% duty cycle for both diodes, indicating balanced operation under resonant conditions. The sharp turn-on and turn-off slopes suggest fast switching, likely facilitated by zero-voltage switching (ZVS) or zero-current switching (ZCS) conditions inherent in resonant operation. Notably, both diodes reach zero current before turning off, further supporting the presence of soft switching in the rectifier stage.

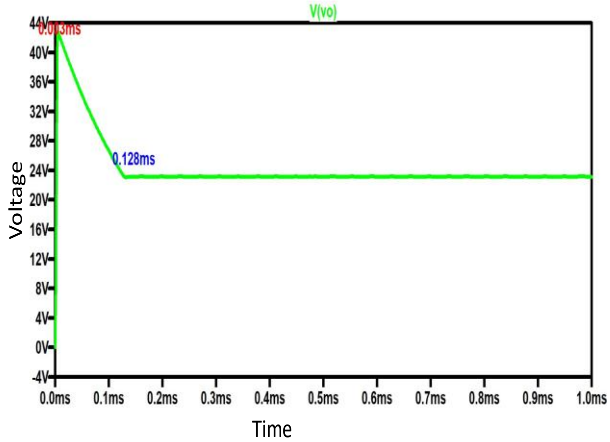

[Fig.10: Output Waveform at Resonant Frequency]

At near-resonant operation, as shown in Figure-9, the output voltage exhibits a slight overshoot (~42-43V) during startup before settling to a well-regulated steady-state of ~23.9V within ~0.128ms. The output shows negligible ripple (<100mV) and delivers a consistent current of ~24A into a 1Ω load, resulting in approximately 573.6W of power. The transient behaviour is smooth without ringing, and although startup is slightly slower than in sub-resonant mode, the exceptionally high efficiency indicates minimised losses due to operation at resonance.

B. Above Resonant Converter (fs=600kHz)

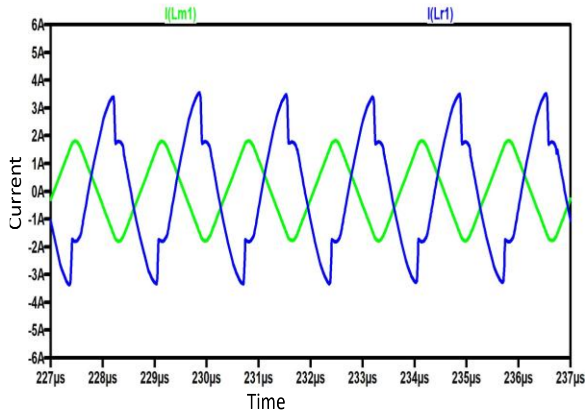

[Fig.11: Inductor's Current Waveform of Converter Above the Resonance Frequency]

At a switching frequency of 600kHz (period ~1.67µs), Both magnetising (I(Lm1)) and resonant (I(Lr1)) inductor currents are shaped by the switching action and resonant tank as shown in Figure 10. I(Lm1) exhibits a triangular-like waveform with rounded transitions, peaking at ±3.4A, while I(Lr1) shows a sinusoidal shape with notches or flattened peaks, reaching ±4.2A. I(Lm1) lags I(Lr1) in phase, indicating that the resonant inductor current responds more quickly as part of the primary resonant path. The consistent frequency confirms the operational setting.

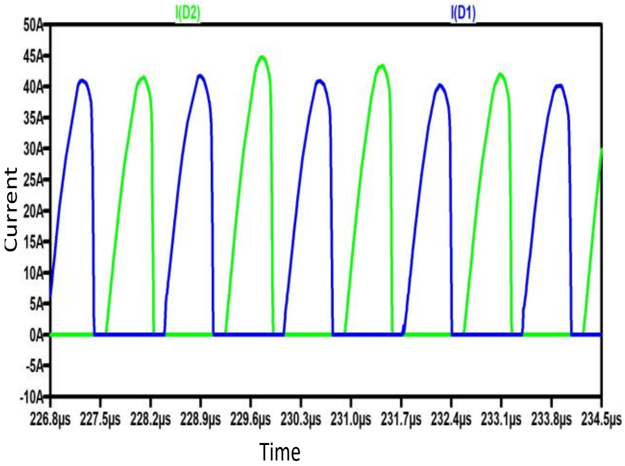

[Fig.12: Diode Waveform of Rectifier above Resonant Converter]

Operating at 600 kHz, diodes D1 (blue) and D2 (green) in the rectifier stage conduct alternately for approximately 833ns per cycle, slightly less than at resonance, as shown in Figure-11. They exhibit increased peak currents ranging from ~42A to 48A. While maintaining a 50% duty cycle and alternating conduction, the turn-on and turn-off slopes are slightly steeper, and there is minimal to no zero current period. This suggests more complex switching and potentially higher switching stress than resonant operation, although current overlap remains minimal.

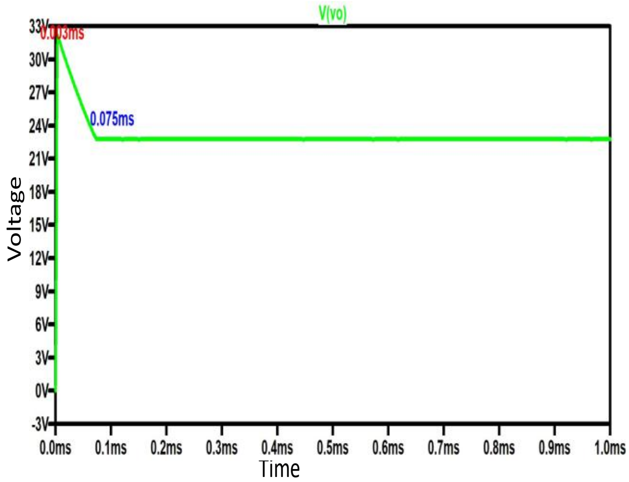

[Fig.13: Output Waveform Above Resonant Frequency]

At above-resonant operation as shown in Figure-12, the output voltage exhibits a slight overshoot (~32-33V) at startup, quickly settling to a well-regulated ~23.9V within ~0.075ms. The ripple remains negligible (<100mV) due to effective filtering. The converter delivers a high output current of ~24A, producing ~573.6W of power. Transient behavior is smooth with minimal overshoot, and startup is rapid. The stable output voltage under heavy load suggests high efficiency, likely exceeding 90%.

C. Below Resonant Converter (fs=300kHz)

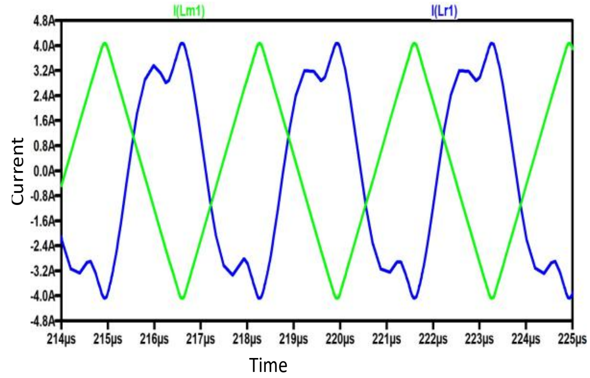

[Fig.14: Inductor's Current Waveform of Converter Below the Resonance Frequency]

Operating below resonance at 300kHz (period ~3.33µs), both magnetizing (I(Lm1)) and resonant (I(Lr1)) inductor currents exhibit distinct waveforms, as shown in Figure-13. The magnetising current is triangular, indicating linear charging and discharging due to a relatively constant voltage, with a peak of ~3.3 A. The resonant current shows a distorted sinusoidal shape, a characteristic of resonant behavior, reaching a higher peak of ~4.5A due to lower impedance at this frequency. Notably, I(Lm1) leads I(Lr1) in phase, a key indicator of operation below the resonant frequency. The consistent frequency confirms the switching frequency setting.

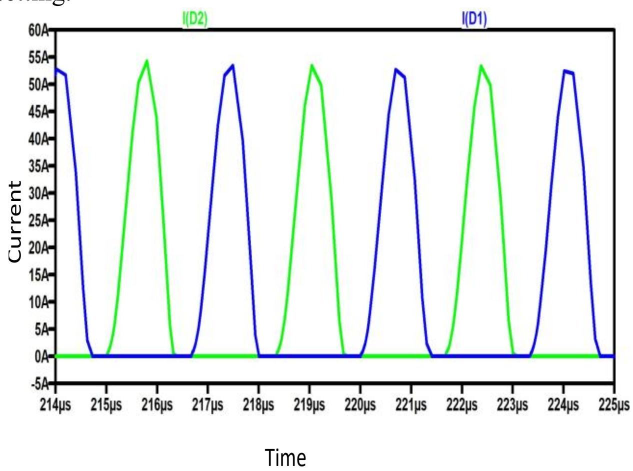

[Fig.15: Diode Waveform of Rectifier Below Resonant Converter]

At a lower switching frequency of 300kHz as shown in Figure-14, diodes D1(blue) and D2(green) conduct alternately for approximately 1.67µs each cycle, a longer duration than observed at higher frequencies. The peak current reaches around 54A, higher than the 42-48A seen at 600kHz, potentially due to the resonant tank's impedance characteristics below resonance. While maintaining a 50% duty cycle and alternating operation, the turn-on and turn-off slopes appear relatively gradual, and there is minimal to no zero current period, suggesting potentially harder switching compared to ideal soft switching conditions.

Retrieval Number:100.1/ijese.G260713070625
DOI:10.35940/ijese.G2607.13070625
Journal Website: www.ijese.org

Published By:
Blue Eyes Intelligence Engineering
and Sciences Publication (BEIESP)

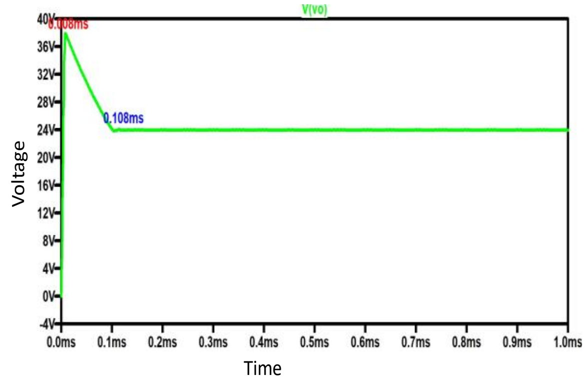

[Fig.16: Output Waveform Below Resonant Frequency]

At the below-resonant operation shown in Figure-15, the startup sequence shows a peak output voltage of ~37V due to initial resonance, quickly settling to a regulated ~23.9V within ~0.1ms. The output exhibits negligible ripple (<100mV), and the converter delivers ~24A into a 1Ω load, resulting in ~573.6W of power. The transient response is smooth with a minor overshoot, and the startup is fast, indicating efficient control. The stable output and low ripple suggest a high efficiency, likely exceeding 90%.

IV. OBSERVATIONS

This section details the observations from the simulation of the LLC resonant converter operating under three distinct frequency conditions relative to the resonant frequency (fr ≈459 kHz): at resonance (fs=fr), above resonance (fs=600 kHz), and below resonance (fs=300 kHz).

A. Inductor Current Waveforms (I(Lm1) and I(Lr1))

A comparison of the magnetizing inductor current (I(Lm1)) and the current flowing through the resonant tank (I(Lr1)) waveforms across the operating modes reveals the following:

Table-II: Comparison of Inductor Current Waveform at Different Regions of Operations

Parameter	At Resonance (fs=459kHz)	Above Resonance (fs = 600 kHz)	Below Resonance (fs = 300 kHz)
Waveform Shape I(Lm1)	Triangular with rounded peaks	Triangular-like	Distinctly triangular
Peak Current I(Lm1)	±2.6A	±3.4A	±3.3A
Waveform Shape I(Lr1)	Sinusoidal with flattened peaks	Sinusoidal with notches/flattened peaks	Distorted sinusoidal
Peak Current I(Lr1)	±3.4A	±4.2A	±4.5A
Phase Relationship	I(Lm1) lags I(Lr1)	I(Lm1) lags I(Lr1)	I(Lm1) leads I(Lr1)
Period	~2.18µs	~1.67µs	~3.33µs
Frequency	459kHz	600kHz	300kHz

Summary of Table 2: The current flowing through the resonant tank (I(Lr1)) consistently shows a more sinusoidal character than the magnetizing inductor current (I(Lm1)), which tends towards triangular. Peak currents vary with frequency, with I(Lr1) peaks generally exceeding I(Lm1) peaks. The phase relationship between I(Lm1) and I(Lr1) serves as a key indicator of the operating mode relative to resonance (lagging above/at resonance, leading below resonance).

B. Output Voltage Waveforms (V(Vo))

The output voltage waveforms demonstrate consistent regulation but differ slightly in transient behavior:

Table-III: Comparison of Output Voltage Waveform at Different Regions of Operations

Parameter	At Resonance (fs = 459kHz)	Above Resonance (fs = 600kHz)	Below Resonance (fs=300 kHz)
Initial Peak Voltage	~42-43V	~32-33V	~37V
Settling Time	~0.128ms	~0.075ms	~0.1ms
Steady-State Voltage	~23.9V	~23.9V	~23.9V
Voltage Ripple	<100mV (negligible)	<100mV (negligible)	<100mV (negligible)
Startup Behavior	Smooth	Quick response	Fast and smooth

Summary of Table 3: Thanks to the output capacitor, the converter achieves excellent output voltage regulation around the target 24 V with minimal steady-state ripple across all modes. The primary difference lies in the startup transient: the settling time is fastest above resonance and slowest at resonance, correlating with the initial voltage overshoot, which is highest at resonance.

C. Diode Current Waveforms

The secondary-side diode currents show significant variation in peak values and conduction characteristics.

Table-IV: Comparison of Diode Current Waveform at Different Regions of Operations

Parameter	At Resonance (fs = 459kHz)	Above Resonance (fs = 600kHz)	Below Resonance (fs = 300kHz)
Conduction Interval per Diode	~1.09 µs	~833ns	~1.67µs
Duty Cycle	~50%	~50%	~50%
Peak Current	~40A	42-48A	~54A
Turn-On/Off Slopes	Sharp slopes	Steeper slopes	More gradual slopes
Switching Condition	ZCS likely (zero current before turn-off)	Possibly harder switching (minimal ZCS)	Hard switching (significant current at turn-off)

Summary of Table 4: Diode conduction remains balanced (~50% duty cycle) across modes. Peak diode currents are highest below resonance and lowest at resonance. The switching characteristics vary significantly: operation at resonance shows signs of soft switching (ZCS). In contrast, operation above and particularly below resonance suggests more complex switching with potentially higher switching losses, as indicated by the non-zero current at turn-off and higher peak currents.

V. CONCLUSION

The simulation results demonstrate the characteristic behavior of an LLC converter operating at, above, and below its resonant frequency.

- **A. Inductor Currents:** The phase relationship between magnetizing and resonant inductor currents clearly distinguishes the operating regime. Current amplitudes vary, with the resonant inductor typically carrying higher peak currents, especially below resonance [5].
- **B. Output Voltage:** Excellent voltage regulation (around 23.9V) is maintained across all modes, with negligible ripple. Transient response varies slightly, with the fastest settling time observed above resonance [3].
- **C. Diode Currents:** The operating frequency significantly affects Peak diode currents, which is the highest below resonance. Operation at resonance offers the most favorable switching conditions (potential ZCS), while deviating from resonance (especially below) leads to harder switching characteristics and higher peak stress on the diodes [2].

These observations align with theoretical LLC converter operation, highlighting the trade-offs between operating frequency, component stresses, and switching losses [1]. Operation near resonance generally provides a good balance, while operation below resonance increases peak currents, and operation above resonance might reduce soft-switching benefits.

ACKNOWLEDGMENT

I would like to express my sincere gratitude to my supervisor, Prof. M.P.S. Chawla, for their invaluable guidance and support—special thanks to Asst. Prof. Khushboo Nagar, thank you for your assistance. Thank you also to the management of SGSITS, Indore (M.P.), for providing the essential resources. I also sincerely appreciate my family & friends' unwavering encouragement throughout this journey.

DECLARATION STATEMENT

After aggregating input from all authors, I must verify the accuracy of the following information as the article's author.

- **Conflicts of Interest/ Competing Interests:** Based on my understanding, this article has no conflicts of interest.
- **Funding Support:** No organisation or agency has sponsored or funded this article. The independence of this research is a crucial factor in affirming its impartiality, as it was conducted without any external influence.
- **Ethical Approval and Consent to Participate:** The data provided in this article is exempt from the requirement for ethical approval or participant consent.
- **Data Access Statement and Material Availability:** The adequate resources of this article are publicly accessible.
- **Author's Contributions:** The authorship of this article is contributed equally to all participating individuals.

REFERENCES

1. Y. Wei, Q. Luo, S. Chen, P. Sun, and N. Altin, "Comparison among different analysis methodologies for LLC resonant converter," IET Power Electronics, vol. 12, no. 9, pp. 2236–2244, 2019, DOI: https://doi.org/10.1049/iet-pel.2019.0027
2. Y. Wei, Q. Luo and H. A. Mantooth, "An LLC Converter With Multiple Operation Modes for Wide Voltage Gain Range Application," in IEEE Transactions on Industrial Electronics, vol.68, no. 11, pp.11111-11124, Nov.2021, DOI: http://doi.org/10.1109/TIE.2020.3029474
3. Samsudin, N. A., & Ishak, D. (2019). Full-bridge LLC Resonant High-voltage DC–DC Converter with Hybrid Symmetrical Voltage Multiplier. IETE Journal of Research, 67(5), 687–698., DOI: https://doi.org/10.1080/03772063.2019.1565954
4. S. Tian, F. C. Lee and Q. Li, "Equivalent circuit modelling of LLC resonant converter," 2016 IEEE Applied Power Electronics Conference and Exposition (APEC), Long Beach, CA, USA, 2016, pp. 1608-1615, DOI: http://doi.org/10.1109/APEC.2016.7468082
5. G. Pledl, M. Tauer and D. Buecherl, "Theory of operation, design procedure and simulation of a bidirectional LLC resonant converter for vehicular applications," 2010 IEEE Vehicle Power and Propulsion Conference, Lille, France, 2010, pp. 1-5, DOI: http://doi.org/10.1109/VPPC.2010.5728978
6. K. Naraharisetti, J. Channegowda and P. B. Green, "Design of Resonant DC-DC LLC converter," 2021 IEEE Kansas Power and Energy Conference (KPEC), Manhattan, KS, USA, 2021 pp.1-6, DOI: http://doi.org/10.1109/KPEC51835.2021.9446206
7. J. F. Lazar and R. Martinelli, "Steady-state analysis of the LLC series resonant converter," APEC 2001. Sixteenth Annual IEEE Applied Power Electronics Conference and Exposition (Cat. No.01CH37181), Anaheim, CA, USA, 2001, pp. 728-735 vol.2, DOI: http://doi.org/10.1109/APEC.2001.912451
8. Y. Hu, J. Shao and T. S. Ong, "6.6 kW High-Frequency Full-Bridge LLC DC/DC Converter with SiC MOSFETs," 2019 IEEE Energy Conversion Congress and Exposition (ECCE), Baltimore, MD, USA, 2019, pp. 6848-6853, DOI: http://doi.org/10.1109/ECCE.2019.8912805
9. Y. Wei, Q. Luo, Z. Wang and H. A. Mantooth, "A Complete Step-by-Step Optimal Design for LLC Resonant Converter," in IEEE Transactions on Power Electronics, vol. 36, no. 4, pp. 3674-3691, April 2021, DOI: http://doi.org/10.1109/TPEL.2020.3015094
10. X. Fang, "Analysis and design optimization of resonant DC-DC converters," Ph.D. dissertation, University of Central Florida, Orlan do, FL, 2012, pp 16-62 Available: http://fpec.ucf.edu/wp-content/uploads/2020/11/Dissertation_Xiang_Fang.pdf
11. T. Hudson, "Understanding LLC Operation (Part I): Power Switches and Resonant Tank," Monolithic Power Systems, Article #A-0028.Rev.1.0,April 2024.[Online].Available:https://media.monolithicpower.com/mps_cms_document/2/0/2022-understanding-llc-operation-part-2-llc-converter-design_r1.0.pdf
12. Infineon Technologies: “Resonant LLC Converter: Operation and Design” Sam Abdel-Rahman, V1.0 September 2012, pp 4-7, Available: Available:https://www.infineon.com/dgdl/Application_Note_Resonant+LLC+Converter+Operation+and+Design_Infineon.pdf?fileId=db3a30433a047ba0013a4a60e3be64a1
13. Mano. (2024, June 17). [LTSPICE] 3kW LLC Resonator Soft Switching. Available: https://youtu.be/plh6mb6SnPg?si=abm9XKPuOPNEmZJY

AUTHOR'S PROFILE

Sushil Bhartoon recently graduated from Shri Govindram Seksariya College of Technology and Science (SGSITS), Indore 452003, India, with a Bachelor of Technology (B. Tech) degree in Electrical Engineering in 2025. His final academic pursuits have ignited a keen interest in the critical aspects of electrical engineering, specifically power quality, electrical machines, power systems, and power electronics. He is eager to leverage this foundational knowledge to contribute to research advancements in this vital area.

Tanmay Dharma is a recent graduate of Shri Govindram Seksariya College of Technology and Science (SGSITS), Indore 452003, India, having earned a Bachelor of Technology (B. Tech) degree in Electrical Engineering in 2025. He has a keen interest in power systems, power electronics, and electrical machines. Power quality is also one of his interests. He is working at SABS Energy Enviro Pvt Ltd. as an energy analyst.

Prof. M.P.S. Chawla, Professor- Ex-Incharge (head), library, Associate Professor in Electrical Engineering Department, SGSITS, Indore-452003 (M.P.)- India, Treasurer IEEE MP Section since Jan 2022, immediate past chairman, 2017- 2018, IEEE M.P. Subsection. He received gold medals in B.E. (Electrical) and M.E. (Power Electronics) degrees from the Electrical Engineering Department at SGSITS, Indore, India, in 1988 and 1992, respectively. He was appointed "Associated Editor in Chief Chair" on 14th December 2018 in Blue Eyes Intelligence Engineering and Sciences Publications, India. His special research interests include power electronics, devices, intelligent instrumentation, biomedical engineering, signal processing, advanced instrumentation systems, soft computing, higher-order statistical techniques, and control systems.

Ms. Khushboo Nagar, Assistant Professor in Electrical Engineering Department since Oct. 2018, SGSITS, 23 Park Road, Indore-452003. She received her Master's Degree in Power Electronics from VITS, Indore 452020 in 2017 and Bachelor's Degree in Electrical and Electronics Engineering from VITS, Indore 452020 in 2015. Her research interests include Power Electronics, HVDC fault detection, Artificial Neural Networks, Power Flow Controllers, Support Vector Machines, and Pattern Recognition.

Retrieval Number:100.1/ijese.G260713070625
DOI:10.35940/ijese.G2607.13070625
Journal Website: www.ijese.org

Published By:
Blue Eyes Intelligence Engineering
and Sciences Publication (BEIESP)